



OPEN ACCESS

EDITED BY
Bryan Briney,
The Scripps Research Institute,
United States

REVIEWED BY
Seth Zost,
Vanderbilt University Medical Center,
United States
Adil Bhat,
University of California, Los Angeles,
United States

*CORRESPONDENCE
Weiqin Li
liweiqindr@nju.edu.cn

SPECIALTY SECTION
This article was submitted to
Vaccines and Molecular Therapeutics,
a section of the journal
Frontiers in Immunology

RECEIVED 07 May 2022
ACCEPTED 07 July 2022
PUBLISHED 09 August 2022

CITATION
Peng M, Dou X, Zhang X, Yan M,
Xiong D, Jiang R, Ou T, Tang A, Yu X,
Zhu F and Li W (2022) Protective
antigenic epitopes revealed by
immun signatures after three doses of
inactivated SARS-CoV-2 vaccine.
Front. Immunol. 13:938378.
doi: 10.3389/fimmu.2022.938378

COPYRIGHT
© 2022 Peng, Dou, Zhang, Yan, Xiong,
Jiang, Ou, Tang, Yu, Zhu and Li. This is
an open-access article distributed under
the terms of the [Creative Commons
Attribution License \(CC BY\)](https://creativecommons.org/licenses/by/4.0/). The use,
distribution or reproduction in other
forums is permitted, provided the
original author(s) and the copyright
owner(s) are credited and that the
original publication in this journal is
cited, in accordance with accepted
academic practice. No use,
distribution or reproduction is
permitted which does not comply with
these terms.

Protective antigenic epitopes revealed by immun signatures after three doses of inactivated SARS-CoV-2 vaccine

Mian Peng^{1,2,3}, Xiaowen Dou⁴, Xiuming Zhang⁴,
Mingchen Yan⁵, Dan Xiong⁴, Ruiwei Jiang⁴, Tong Ou⁴,
Aifa Tang⁶, Xiqiu Yu⁷, Feiqi Zhu⁸ and Weiqin Li^{1,2*}

¹The First School of Clinical Medicine, Southern Medical University, Guangzhou, China, ²Department of Critical Care Medicine, Affiliated Jinling Hospital, Medical School of Nanjing University, Nanjing, China, ³Department of Critical Care Medicine, The Third Affiliated Hospital of Shenzhen University, Shenzhen, China, ⁴Medical Laboratory, The Third Affiliated Hospital of Shenzhen University, Shenzhen, China, ⁵Department of Artificial Intelligence and Bioinformatics, Shenzhen Digital Life Research Institute, Shenzhen, China, ⁶Science and Education Center, The Third Affiliated Hospital of Shenzhen University, Shenzhen, China, ⁷Department of Gastroenterology, The Third Affiliated Hospital of Shenzhen University, Shenzhen, China, ⁸Department of Neurology, The Third Affiliated Hospital of Shenzhen University, Shenzhen, China

Background: SARS-CoV-2 (severe acute respiratory syndrome coronavirus 2) has infected millions of people around the world. Vaccination is a pillar in the strategy to control transmission of the SARS-CoV-2 spread. Immune responses to vaccination require elucidation.

Methods: The immune responses to vaccination with three doses of inactivated SARS-CoV-2 vaccine were followed in a cohort of 37 healthy adults (18–59 years old). Blood samples were collected at multiple time points and submitted to peptide array, machine learning modeling, and sequence alignment analyses, the results of which were used to generate vaccine-induced antibody-binding region (VIABR) immun signatures (Registration number: ChiCTR2200058571).

Results: Antibody spectrum signals showed vaccination stimulated antibody production. Sequence alignment analyses revealed that a third vaccine dose generated a new highly represented VIABR near the A570D mutation, and the whole process of inoculation enhanced the VIABR near the N501Y mutation. In addition, the antigen conformational epitopes varied between short- and long-term samples. The amino acids with the highest scores in the short-term samples were distributed primarily in the receptor binding domain (RBD) and N-terminal domain regions of spike (S) protein, while in the long-term samples (12 weeks after the 2nd dose), some new conformational epitopes (CEs) were localized to crevices within the head of the S protein trimer.

Conclusion: Protective antigenic epitopes were revealed by immunosignatures after three doses of inactivated SARS-CoV-2 vaccine inoculation. A third dose results in a new top-10 VIABR near the A570D mutation site of S protein, and the whole process of inoculation enhanced the VIABR near the N501Y mutation, thus potentially providing protection from strains that have gained invasion and immune escape abilities through these mutation.

KEYWORDS

protective antigenic epitopes, immunosignatures, three doses, inactivated, SARS-CoV-2 vaccine

Background

SARS-CoV-2 (severe acute respiratory syndrome coronavirus 2) is the highly pathogenic virus that caused the COVID-19 (coronavirus 2019) pandemic following its emergence in late 2019. Its emergence followed two other newly identified highly pathogenic coronaviruses, namely those that caused the Middle East respiratory syndrome and original SARS outbreaks in the late 20th and early 21st centuries, respectively (1). An effective vaccine is considered to be essential for limiting SARS-CoV-2 transmissibility and for protecting against severe COVID-19 morbidity and mortality (2). Most of the current COVID-19 vaccine research focuses on virus-vectored vaccines or mRNA vaccines (3–6). So far, there have been limited studies on inactivated SARS-CoV-2 vaccines.

The efficacy of Sinovac's inactivated SARS-CoV-2 vaccine (ISC2V) is being examined in an ongoing clinical trial of healthcare professionals with the incidence of symptomatic virologically confirmed COVID-19 cases two or more weeks after the second vaccination serving as the primary efficacy endpoint. Results from this trial have not yet been published (7). A prior report of the findings of phase 1 and phase 2 ISC2V trials conducted in China showed low adverse reaction rates and demonstrated immunogenicity, leaving questions regarding efficacy and possible long-term adverse events for phase 3 trials (8). The epitopes that antibodies generate in response to inactivated SARS-CoV-2 vaccine target have not yet been

reported. The aims of the present study were firstly to examine the immune efficacy of ISC2V in terms of its ability to induce human immune spectrum changes and secondly to identify the antigenic epitopes of vaccine action by way of immunosignatures developed based on peptide array technology.

Methods

Participants

A cohort of 37 healthy adults who agreed to receive three ISC2V doses were recruited into the study. The inclusion criteria were: being 18–59 years old; having negative nucleic acid detection and specific IgM, IgG SARS-CoV-2 tests; being in good health without any known underlying diseases; ISC2V acceptance; and not having a serious adverse reaction during vaccination with ISC2V (9). The exclusion criteria beyond not meeting the aforementioned inclusion criteria were: being pregnant or becoming pregnant during follow-up (including miscarriage/abortion); suffering an acute illness requiring hospitalization during follow-up; and choosing to withdraw from the study for any reason. Written informed consent was obtained from each participant prior to commencement of the study. Ethics approval was obtained from the Ethics Committee of the Third Affiliated Hospital of Shenzhen University.

Experimental timepoints

The data were analyzed over nine time points, with each time point being defined relative to the most recent prior vaccine injection, including whether it was the first, second, or third vaccine dose (indicated as Injection I, II, or III) and how many weeks (indicated as 2w, 4w, 12w, 24w, or 32w) have passed since that most recent injection. Thus, the nine study time points were: Injection I-2w; Injection I-4w; Injection II-2w; Injection II-4w; Injection II-12w; Injection II-24w; Injection II-32w; Injection

Abbreviations: AUC, area under the curve; BMI, body mass index; CE, conformational epitope; COVID-19, coronavirus disease 2019; ISC2V, Sinovac's inactivated SARS-CoV-2 vaccine; FDR, false discovery rate; FG, original data foreground; Nab, neutralizing antibody; PBSTP, phosphate buffered saline with 0.05% Tween20 and 0.1% ProClinTM; RBD, receptor binding domain; ROC, receiver operating characteristic; S, spike; SARS-CoV-2, severe acute respiratory syndrome coronavirus 2; SDP, significantly differentiated peptide; VIABR, vaccine-induced antibody-binding region.

III-2w; and Injection III-4w. Naïve immunity baseline data for comparison are referred to as Injection I-0 data. Additionally, the Injection I-4w and Injection II-32w time points served as baseline reference data for Injection II and Injection III, respectively, at which times they are referred to as Injection II-0 and Injection III-0, respectively.

Descriptive data

The following data were collected for each participant: gender, age, height (cm), body weight (kg), disease history, ISC2V injection dates, and any local or systemic adverse reactions after each injection.

Biological sample preparation

At each time point, 1 ml of whole blood was drawn from each subject and centrifuged at 3500 RPM for 5 min. The upper serum fraction was taken and stored at -80°C . Sample aliquots were thawed at 4°C and 3 μl of each sample was diluted 1:25 in 72 μl mannitol buffer [1% mannitol in PBSTP (phosphate buffered saline with 0.05% Tween20 and 0.1% ProClinTM); ingredients from Sigma-Aldrich, USA]. Then, 5- μl aliquots of the 1:25 sample dilutions were transferred into the 96-well plates (Axygen Scientific, Union City, CA), where they were combined with 120 μl of PBSTP to produce 1:625 dilutions for use in the assay.

Peptide assays

Peptide arrays were rehydrated by soaking in distilled water for 20 min. Rehydrated arrays were sprayed three times briefly with 90% isopropanol (Thermo Fisher Scientific, USA) ensuring full coverage, centrifuged to remove excess liquid, and then loaded into a peptide array cassette. Each sample was diluted 1:625 in mannitol buffer (1% mannitol in PBSTP), and then 90 μl of the diluted sample was transferred to the cassette. To facilitate antibody-peptide binding, the mixture was incubated on the arrays for 1 h at 37°C while shaking on a TeleShake95 shaker (INHECO, Martinsried, Germany). Subsequently, the cassette was washed 10 times in PBSTP with a BioTek 405TS microplate washer (BioTek Instruments, Winooski, VT, USA). Bound antibody was detected by adding 4 nM goat anti-human IgG (H+L) secondary antibody coupled to AlexaFluor 555 (Thermo Fisher Scientific, USA) in secondary incubation buffer [0.75% casein (Sigma-Aldrich, USA) in PBSTP] for 1 h at 37°C shaking on a TeleShake95 shaker. After incubation with the secondary antibody, the peptide arrays were again washed with PBSTP, followed by a rinse in distilled water. After being removed from the cassette, the peptide arrays were sprayed with

90% isopropanol and excess liquid was removed by centrifugation at 3000 RPM for 60 s.

Data acquisition and processing

Peptide arrays were scanned individually in an ImageXpress Micro 4 imaging system (Molecular Devices, Santa Clara, CA), which generated TIFF images. The images were analyzed in MIAMI software wherein an automated grid algorithm was applied to identify areas associated with each peptide, yielding a GPR5 format data matrix. The original data foreground (FG) of each polypeptide was extracted from the data matrix in GPR5 format. Because the original fluorescence signal data show a lognormal distribution, log-FG was obtained by logarithmic transformation after adding the constant 100 to the FG to improve homovariance. Data measurement accuracy was roughly proportional to intensity. The median of all peptides in each array was subtracted from the peptide signal log-FG to obtain a normalized log-FG.

Difference analysis of peptide signal

At each sampling time point, each peptide signal (features of normalized log-FG) was ranked according to its p value in a t -test relative to baseline (pre-vaccination) levels. A 5% false discovery rate (FDR) threshold that distinguished clearly between before and after vaccination states was applied and those peptides with a significant difference whose fold-change of the original signal was greater than 1 after vaccination were identified as significantly differentiated peptides (SDPs). If the number of peptides reaching the threshold was less than 100, then the top 1000 peptides with the lowest p values were selected as SDPs.

Polypeptide sequence alignment scoring

To reveal potential epitopes of vaccine action, SDP sequences were aligned with Spike (S) protein sequences obtained from a SARS-CoV-2 reference proteome (National Center for Biotechnology Information, NC_045512) (10) via Basic Local Alignment Search Tool (BLAST) analysis (seed 3, gap penalty 4), and the scoring matrix BLOSUM62 was adjusted according to the amino acid composition of the peptide arrays (11). Each reference sequence area was aligned with a group of SDPs. The sum of all aligned SDPs within an area served as an amino acid score, a . To correct for array composition deviation, we use the same method to calculate the background score, b , of all peptide arrays in the location. The number of SDPs screened out was recorded as c , and the number of all peptide arrays was recorded as d . Each final score, s , was calculated as follows: $s = a$

– $(c/d) \times b$. Total scores of 20-mer sequence spans were obtained by window sliding. The top-10 total scores for non-overlapping S protein sequence spans were accepted as linear vaccine-induced antibody-binding regions (VIABRs).

Patch-based conformational epitope identification

After obtaining the complete spatial structure file for S Protein from <https://charmm-gui.org> (12), the Dictionary of Secondary Structure of Protein (13, 14) was used to analyze S Protein Structure and to calculate the relative surface accessibility of each residue. Residues on the protein surface were obtained according to the residual relative surface accessibility, and overlapping residue-centered patches were generated. SDPs were aligned with the patches based on maximal bipartite matching in a bipartite graph, and alignment scores were calculated with the aa similarity matrix (15–17). Post-processing (clustering, merges, and gap filling) were carried out according to alignment scoring to obtain candidate CE information. Visualization of CEs relative to protein spatial structure was conducted in Pymol software.

Consistency analysis with SARS-CoV-2 neutralizing antibodies

The amino acid composition of each CE was compared with that extracted from the binding site of each SARS-CoV-2 neutralizing antibody (downloaded from the immune epitope database). When there was >80% amino acid identity, a sequence was considered to match a neutralizing antibody CE. The identity of each thus matched CE was recorded.

Scoring model

Because machine learning modeling requires sample training to follow the principle of independent and identical distribution, we set up antibody level scoring models separately for short-term samples and long-term samples. In the short-term sample scoring model, sample pools within 4 weeks after each inoculation (Injection I-2w; Injection I-4w; Injection II-2w; Injection II-4w; Injection III-2w; and Injection III-4w) were used as training-set case samples. In the long-term sample scoring model, sample pools beyond 4 weeks (Injection II-12w; Injection II-24w; and Injection II-32w) were used as training-set case samples. The Injection I-0 (prevaccination) sample was used as a baseline control for both models. Dichotomous predictions were performed, and the predicted probabilities were used as antibody level scores. A Venn diagram was made to identify which peptide signals were shared and which were not shared between long-term and short-

term samples. The leave-one-out method, enhanced to adjust to queue characteristics, was used to prevent information leakage consequent to the donor data distributions of the training and test sets. Logistic regression was used to construct the classification model. Receiver operating characteristic (ROC) curves were produced for each model and the area under the curve (AUC) was determined for each ROC curve.

Statistical analysis

Data processing and hypothesis testing were performed in R3.6 and Python3.7. Differences in model prediction scores between samples of different sampling points were calculated with *t*-tests. Differences with a *P* value <0.05 were considered significant.

Results

Baseline characteristics of the participants

A total of 37 participants (23 women and 14 men) were enrolled. They had a median (\pm standard deviation) age of 32.51 ± 6.50 years and body mass index (BMI) of 21.71 ± 3.24 kg/m², respectively. The age, height, weight, and BMI for each participant are shown in Table 1. All 37 participants followed a three-injection ISC2V inoculation protocol with a 4-week interval from the first to the second injection and a 32-week interval from the second to the third injection. None of the participants had preexisting diseases or severe adverse reactions to ISC2V inoculation.

Vaccine antibody response-associated polypeptides

After sample processing and data acquisition, 100–5000 SDPs were identified at each time point. Volcano plots (Figure 1) were produced to illustrate the significance of differences across time points as a function of the ratio of means of each post-inoculation peptide array across the experimental time points relative to the pre-inoculation baseline. Notably, SDPs with ratio values greater than 1 were observed for every inoculation-timepoint group and larger ratios tended to have more statistically significant differences, suggesting that inoculation can promote the production of effector antibodies.

Sequence alignment

Following alignment of vaccine-induced antibody response-associated SDPs at each sampling time point with reference-

TABLE 1 Baseline data for each participant.

	Gender	Age(years)	Height(cm)	Weight(kg)	BMI(kg/m ²)
C1	Female	31	163	50	18.82
C2	Female	36	164	54	20.08
C3	Female	28	164	50	18.59
C4	Female	24	163	47	17.69
C5	Female	32	159	52	20.57
C6	Female	27	157	50	20.28
C7	Male	31	173	65	21.72
C8	Female	26	157	50	20.28
C9	Female	32	160	51	19.92
C10	Female	27	157	50	20.28
C11	Male	36	173	65	21.72
C12	Male	31	172	60	20.28
C13	Male	32	169	60	21.01
C14	Male	45	175	70	22.86
C15	Female	28	162	55	20.96
C16	Female	30	158	50	20.03
C17	Female	55	160	47	18.36
C18	Male	30	172	78	26.37
C19	Male	29	187	105	30.03
C20	Female	27	165	55	20.20
C21	Male	48	170	65	22.49
C22	Female	33	163	60	22.58
C23	Female	38	155	60	24.97
C24	Female	32	161	50	19.29
C25	Female	33	153	48.5	20.72
C26	Female	43	160	60	23.44
C27	Female	33	158	55	22.03
C28	Female	27	155	60	24.97
C29	Male	26	160	70	27.34
C30	Male	33	183	75	22.30
C31	Male	27	174	65	21.47
C32	Female	28	165	50	18.37
C33	Male	32	174	100	33.03
C34	Female	30	162	50	19.05
C35	Male	31	168	55	19.49
C36	Male	39	170	60	20.76
C37	Female	33	155	50	20.81

proteome SARS-CoV-2 S protein sequences, the top-10 total scores for non-overlapping 20-mer amino acid-sequence spans from the S protein were identified as linear VIABRs (highlighted in [Figure 2A](#)). The three-dimensional structure positions of A570 and N501 are shown in [Figure 2B](#).

Following alignment of the spatial structure of SDPs with those of the SARS-CoV-2 S protein, we identified 6~8 corresponding CEs at each time point. Each identified CE is composed of 12~41 aa which are discontinuous in sequence but relatively close in space. The CEs of the receptor binding domain (RBD) are shown in [Figure 2C](#).

Peptide array-based antibody level scoring

The SDPs that were unique identified to each phase of the inoculation protocol are shown in a Venn Diagram in [Figure 3](#). In the post-injection I period and in the post-injection III period, we identified 1,172 and 113 unique SDPs, respectively. Altogether, there were 2,089 SDPs unique to the post-Injection II period, only 218 of which were found for *both* the short-term and long-term samples. Of the remaining 1,871 SDPs from this period, 222 were unique to the long-term samples while 1,649

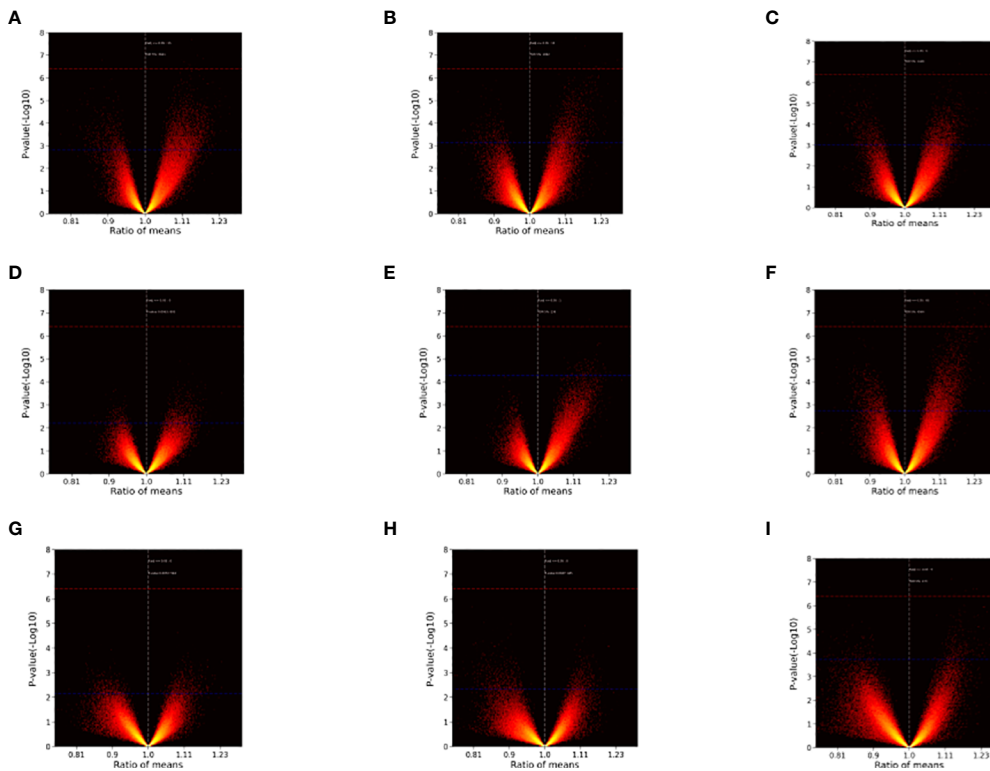


FIGURE 1
 Volcano plots illustrating inter-group differences. **(A)** Injection I-2w vs. Injection I-0. **(B)** Injection I-4w vs. Injection I-0. **(C)** Injection II-2w vs. Injection I-0. **(D)** Injection II-4w vs. Injection I-0. **(E)** Injection II-12w vs. Injection I-0. **(F)** Injection II-24w vs. Injection I-0. **(G)** Injection II-32w vs. Injection I-0. **(H)** Injection III-2w vs. Injection I-0. **(I)** Injection III-4w vs. Injection I-0. The ratio of means for each peptide array post-inoculation across different time points relative to the baseline are shown on the x-axes. The significance of the comparisons [p value (-Log 10)] is represented on the y-axes. Red dashed lines indicate Bonferroni-corrected $p = 0.05$ threshold. Blue dashed lines indicate 5% FDR boundary. Note that ratios with greater (absolute) values tended to be more significant and differences (ratio > 1) emerged at every time point.

were unique to the short-term samples (FDR = 0.05). Only 72 SDPs were common throughout the entire immunization cycle, indicating that the long- and short-term samples showed different antibody binding patterns.

The short-term sample model (Figure 4A), whose ROC had an AUC of 0.88 (Figure 4B), had a baseline sample score of ~0.25, while the post-inoculation scores exceeded 0.65. Scores increased gradually with time after the inoculation until they reached maximum levels at the Injection II-2w time points. By the Injection II-4w time point, the scores decreased to 0.65. Subsequently, scores increased gradually until the Injection III-4w time point, when they reached levels similar to that seen at Injection II-2w.

The long-term sample model (Figure 4C), whose ROC had an AUC of 0.62 (Figure 4D), showed that the score distribution at the Injection II-12w time point skewed to slightly greater values than those observed at baseline and then proceeded to decrease at subsequent time points (Injection II-24w and -32w), indicating that some antibodies were still being produced 12

weeks after inoculation, though these signals were trending toward a state of extinction.

Classification of immune responses based on antibody level scoring of polypeptide arrays

In the short-term model, the 37 participants could be divided into four reaction types based on k-means clustering (Figure 5A): Type 1 (N = 17), Type 2 (N = 6), Type 3 (N = 8), and Type 4 (N = 6). The Type 1 individuals had strong vaccine antibody responses indicative of vaccine effectiveness. The Type 2 individuals had weak antibody responses initially but then achieved high antibody level scores after the third injection. Type 3 and 4 were characterized by fluctuating responses over the inoculation course, with Type 3 individuals exhibiting a lasting response to the first injection, while Type 4 showed more robust responses to booster injections than to the first injection.

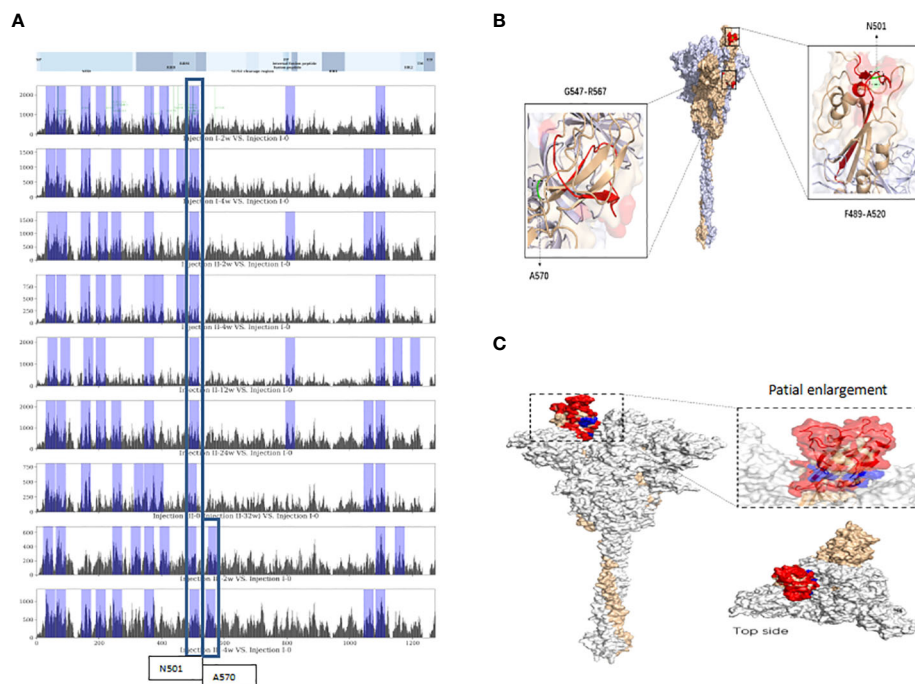


FIGURE 2

Linear and conformational epitopes identified following sequence alignment. (A) Top-10 scoring sequence spans in protein S (non-overlapping) at each assessment time point located near N501 or A570. (B) Three-dimensional structure positions of A570 and N501. (C) The CEs of the RBD. Red-highlighted aa residues were consistent spatial epitopes across all timepoints, and those marked in blue are located within the crevices of the spatial structure of the head of the S-protein trimer and were observed in long-term sample analyses (12 weeks after the 2nd dose).

Analysis of the demographic characteristics showed that men and women had similar age distributions across the four types (Figure 5B). However, Type 2 (initially poor responder) individuals tended to have high BMIs, among both men and women, though the effect was more pronounced in men than in women (Figure 5C).

Discussion

SARS-CoV-2, which emerged in China in late 2019, has infected millions of people around the world, achieving a much greater infection reach than previously known coronaviruses (18). As of the summer of 2022, the COVID-19 pandemic represented the sixth time the WHO had declared a global emergency following the H1N1 swine flu in 2009, Ebola (West Africa) in 2013, polio in 2014, Zika in 2016, and Ebola (Democratic Republic of Congo) in 2019 (19). Given the epidemiology of COVID-19, efficacious vaccination remains essential to minimizing COVID-19 morbidity and mortality.

The WHO recognizes seven COVID-19 vaccine strategies: inactivated virus; virus-like particle or nanoparticle; protein subunit; virus-vector; DNA; mRNA; and live-attenuated virus (20). Among them, particularly supportive data have

been reported for ChAdOx1, a virus-vector vaccine, and BNT162b2, an mRNA vaccine. Notably, interim analyses of randomized controlled trials of ChAdOx1 in the UK, South Africa, and Brazil have affirmed an acceptable safety profile with good efficacy in adults (6). In another report in the UK, both ChAdOx1 and BNT162b2 were reported to produce anti-S protein IgG responses in large adult population samples, though the responses differed in relation to the number of doses received, age, gender, and long-term health conditions (21). A sentinel surveillance study conducted in Chile with 56,261 vaccinated adults showed that, compared to that in BNT162b2-inoculated participants, IgG seropositivity obtained after vaccination with CoronaVac, an inactivated virus vaccine, was lower and tended to decline more quickly (22). Because immune responses to different vaccine types and doses differ, and there are limited ISC2V studies, we could not have predicted the course of immunity acquisition that people would show over the course of receiving three doses of ISC2V inoculation. The presently identified SDPs provide information that may be useful for elucidating the mechanisms of ISC2V inoculation.

The conventional techniques that are used to assess immunogenicity and immune responses are analyses of neutralizing antibodies (NAbs). Previously, we have observed good concordance (>0.78) between conventional virus

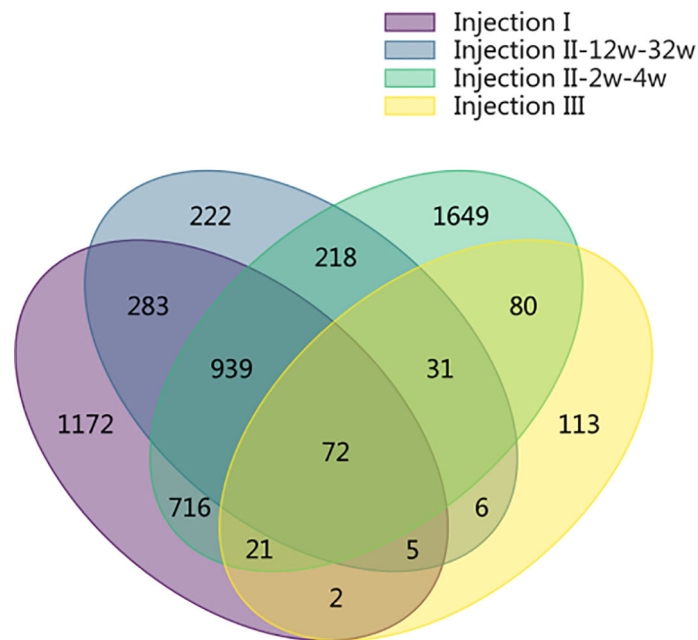


FIGURE 3

Venn diagram showing the SDPs that were unique identified to each phase of the inoculation protocol. In the post-injection I period and in the post-injection III period, we identified 1,172 and 113 unique SDPs, respectively. Altogether, there were 2,089 SDPs unique to the post-Injection II period, only 218 of which were found for both the short-term and long-term samples. Of the remaining 1,871 SDPs from this period, 222 were unique to the long-term samples while 1,649 were unique to the short-term samples (FDR = 0.05). Only 72 SDPs were common throughout the entire immunization cycle, indicating that the long- and short-term samples showed different antibody binding patterns.

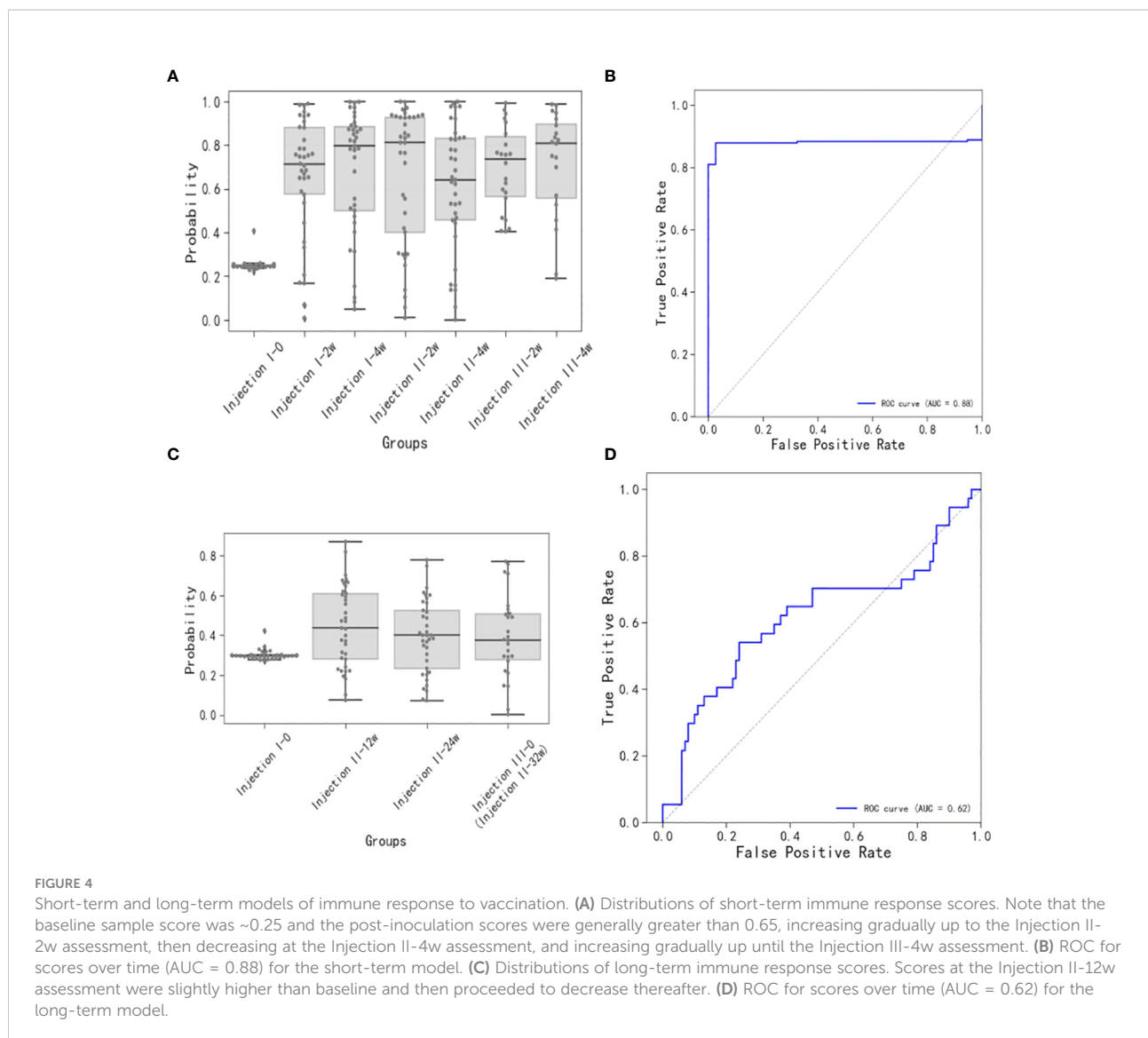
neutralization test and enzyme linked immunosorbent assay NAb results. Although NAb titers were found to decrease gradually after ISC2V vaccination in our prior work, the seropositive rate of NAb remained at 84% over 6 months of observation (23). Notably, although NAb assays based on competitive binding of angiotensin-converting enzyme 2 with the RBD remain the classic immunity marker, peptide arrays are measuring features of the response that are not measured in conventional neutralization assays. Studies using different techniques to evaluate vaccines provide more profound understanding of the vaccines and remain to be the focus of future work for the field.

Peptide microarray-based immunosignature technology captures epitope-binding of antibody immune spectrum signals and displays antibody diversity, thus providing broad information regarding circulating antibody repertoires. Using this technique, Arvey et al. characterized serum antibody binding to high-density peptide microarrays with samples from a diverse cohort of 1,675 subjects and found that the circulating antibody repertoires of older subjects showed particularly robust binding to thousands of di-serine peptide-containing peptides, which can be attributed to immune age (24). The sequence peptides are analyzed at a high density and their analysis yields CEs, which are key to evaluating vaccines, in addition to linear epitopes.

Given the difficulties inherent in producing properly folded proteins, peptide arrays are an alternative means of defining antibodies to CEs (25–27). In a study in which full reactivity profiles of vaccine-generated antibodies were produced, Legutki et al. found an antibody that was common to COVID-19 survivors while being absent in those who died (28). In the present study, by comparing immune spectra between vaccinated and non-vaccinated samples, we were able to identify SDPs as potentially relevant epitope sites. We were then able to identify and rank putative epitopes according to SDP enrichment and thus identify those most likely to be related to a SARS-CoV-2 antigen epitope.

Our linear sequence alignment analysis revealed that those sequence spans that aligned best with the S protein sequence are distributed predominantly in the RBD and N-terminal domain regions. These two regions have important functions related to viral invasion of host cells (29), and they have been shown to be the most common binding targets of SARS-CoV-2 neutralizing antibodies (30, 31). Notably, most escape mutations, including those in the UK variant B.1.1.7, Delta strains, and Omicron strains of SARS-CoV-2, have been reported to occur within these two regions (32–34).

The intersections of our top-10 S protein VIABRs with the key amino acid spans of known neutralizing antibodies published by La Jolla Institute for Immunology (LJI) (35) may



be used as references for the design of polypeptide or optimized-subunit vaccines. After the third ISC2V injection, a new top-10 VIABR intersecting with a region published by LJI emerged. Near that VIABR, there is an A570D mutation, which has been shown to reduce contact between individual chains of the trimeric S protein protomer, potentially enhancing cleavage into S1 and S2 subunits, dynamic structural rearrangement, and host cell fusion mechanisms in the UK variant B.1.1.7 (36–39). The epitope region near A570 is located in a loop at beta-sheet junction (see three-dimensional structure of A570 shown in Figure 2B). An A570 mutation that changes antibody binding with this local structure may underlie the variation in UK Variant B.1.1.7. The fact that this VIABR is located entirely within the beta sheet suggests that a vaccine-enhanced VIABR may be protective against the UK Variant B.1.1.7.

In addition, we found a top-10 VIABR in the N501Y mutation region that persisted throughout the inoculation course of three ISC2V injections. This particular mutation has been identified as being pathogenically important in a number of strains due to its producing enhanced virus invasion and immune escape (40–42). This finding suggests that ISC2V may provide antibody protection against Delta and Omicron variants. Additionally, these data indicate that a three-dose ISC2V strategy may provide highly comprehensive protection, including against novel SARS-CoV-2 strains.

In the result, we documented distinct short- versus long-term immune response patterns following ISC2V injections. In the short term, vaccinated participants showed antibody responses that peaked about 2 weeks after the second injection and about 4 weeks after the third injection. In the long term, antibody levels

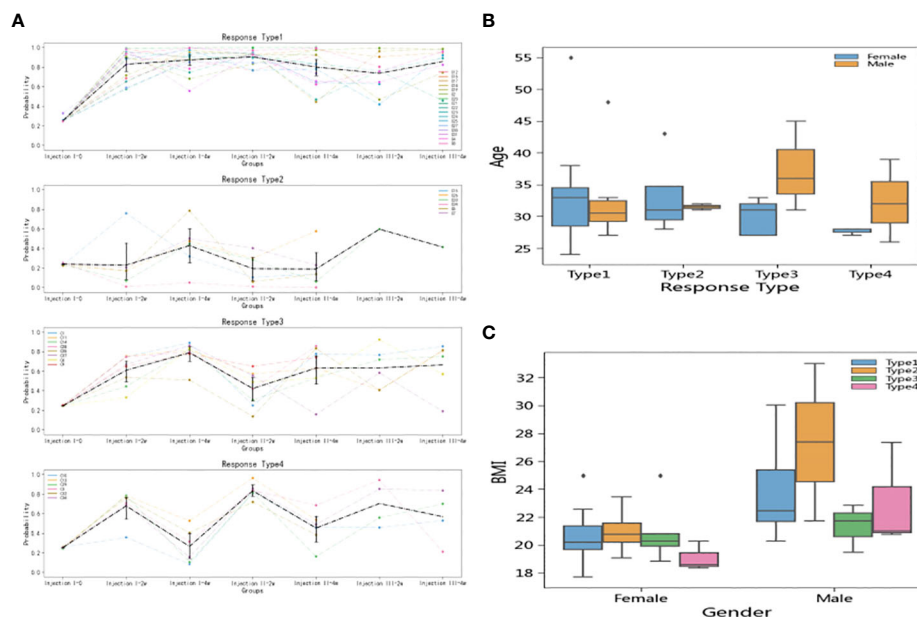


FIGURE 5

Inoculation reaction types and relationship of types to individual factors. (A) Types were defined according to k-means clustering, with Type 1 showing strong antibody responses, Type 2 showing weak responses until the third dose, Type 3 showing a lasting response to the first dose, and Type 4 showing a notable boosts in immune response to follow-up doses. (B) There was no significant difference between the age distributions of men and women in terms of vaccine response. (C) Type 2 participants (poor responders to doses 1 and 2) had higher BMI values than participants in the other type groups. The effect was significant in both women and men, but dramatically more pronounced in men than in women.

showed slight increases 12 weeks after the second dose and then decreased gradually from then onward. Interestingly, antigen epitopes varied between short- and long-term samples. Our alignment CE analysis showed that the highest-scoring amino acid spans in the short-term samples were distributed primarily in the RBD and NTD regions of the S protein. Meanwhile, in long-term samples (12 weeks after the 2nd dose), some new CEs were identified within the crevices of the spatial structure of the head of the S protein trimer. Thus, the long-term immunogenic effects of ISC2V may contribute to the generation of antibodies that bind to the gaps of S-protein-trimer RBD. These antibody binding pattern differences between short-term and long-term samples suggest that there is a strong short-term RBD antibody response that diminishes over time, perhaps limited by the B cell lifespan (43–45), while long-lived plasma cells produce multiple antibodies with different binding modes (46, 47). Our polypeptide array experiments also showed that vaccination can stimulate antibody production in both the short term (within 4 weeks) and the long term (beyond 4 weeks), which is consistent with prior findings obtained by Xia et al. with the inactivated SARS-CoV-2 vaccine BBIBP-CORV 27 (48), wherein humoral responses against SARS-CoV-2 were observable in all examined vaccine recipients 42 days after inoculation.

Our follow-up analyses of immune response types based on short-term model scores indicated that high-BMI individuals,

especially men, were most likely to have a weak antibody production response to the vaccine (Type 2 short-term model outcome). Prior studies have provided evidence of a linear dose-response association of BMI with COVID-19 severity and mortality. Likewise, obesity per se (BMI ≥ 30 kg/m²) has been shown to be a risk factor for critical COVID-19 and in-hospital mortality due to COVID-19 (49–51). Although we did not observe a statistically significant correlation between BMI and vaccine efficacy in our study, it would be of interest to further determine whether obese individuals would benefit from augmented vaccine exposure relative to the general population.

This article has a notable limitation in that only 37 individuals were represented in the results. A larger population of participants will be required to further confirm the present findings and conclusions.

Conclusion

ISC2V inoculation stimulates antibody production. After the third dose, a new top-10 VIABR was generated near the A570D mutation site of the viral S protein. A VIABR near the N501Y mutation was enhanced throughout the three-injection inoculation course. Three doses of ISC2V may provide more

comprehensive antibody protection against novel variants of SARS-CoV-2 than is obtained with only two doses.

Data availability statement

The raw data supporting the conclusions of this article will be made available by the authors, without undue reservation.

Ethics statement

This study was reviewed and approved by The Ethics Committee of the Third Affiliated Hospital of Shenzhen University. The patients/participants provided their written informed consent to participate in this study.

Author contributions

MP was a major contributor in designing the study and writing the manuscript. XD, XZ, and MY helped with the design of the study. AT, XY and FZ collected the data. DX, RJ and TO analysed and interpreted the data. WL designed the study and revised the article. All authors contributed to the article and approved the submitted version.

References

- Guo YR, Cao QD, Hong ZS, Tan YY, Chen SD, Jin HJ, et al. The rigin, transmission and clinical therapies on coronavirus disease 2019 (COVID-19) outbreak - an update on the status. *Mil Med Res* (2020) 7(1):11. doi: 10.1186/s40779-020-00240-0
- Hodgson SH, Mansatta K, Mallett G, Harris V, Emary KRW, Pollard AJ. What defines an efficacious COVID-19 vaccine? a review of the challenges assessing the clinical efficacy of vaccines against SARS-CoV-2. *Lancet Infect Dis* (2021) 21(2):e26–35. doi: 10.1016/S1473-3099(20)30773-8
- Jackson LA, Anderson EJ, Roupheal NG, Roberts PC, Makhene M, Coler RN, et al. An mRNA vaccine against SARS-CoV-2 - preliminary report. *N Engl J Med* (2020) 383(20):1920–31. doi: 10.1056/NEJMoa2022483
- Mulligan MJ, Lyke KE, Kitchin N, Absalon J, Gurtman A, Lockhart S, et al. Phase I/II study of COVID-19 RNA vaccine BNT162b1 in adults. *Nature* (2020) 586(7830):589–93. doi: 10.1038/s41586-020-2639-4
- Folegatti PM, Ewer KJ, Aley PK, Angus B, Becker S, Belij-Rammerstorfer S, et al. Safety and immunogenicity of the ChAdOx1 nCoV-19 vaccine against SARS-CoV-2: a preliminary report of a phase 1/2, single-blind, randomised controlled trial. *Lancet* (2020) 396(10249):467–78. doi: 10.1016/S0140-6736(20)31604-4
- Voysey M, Clemens SAC, Madhi SA, Weckx LY, Folegatti PM, Aley PK, et al. Safety and efficacy of the ChAdOx1 nCoV-19 vaccine (AZD1222) against SARS-CoV-2: an interim analysis of four randomised controlled trials in Brazil, south Africa, and the UK. *Lancet* (2021) 397(10269):99–111. doi: 10.1016/S0140-6736(20)32661-1
- Palacios R, Patiño EG, Piorelli RO, Conde MTRP, Batista AP, Zeng G, et al. Double-blind, randomized, placebo-controlled phase III clinical trial to evaluate the efficacy and safety of treating healthcare professionals with the adsorbed COVID-19 (Inactivated) vaccine manufactured by sinovac - PROFISCOV: A structured summary of a study protocol for a randomised controlled trial. *Trials* (2020) 21(1):853. doi: 10.1186/s13063-020-04775-4
- Xia S, Duan K, Zhang Y, Zhao D, Zhang H, Xie Z, et al. Effect of an inactivated vaccine against SARS-CoV-2 on safety and immunogenicity outcomes: Interim analysis of 2 randomized clinical trials. *JAMA* (2020) 324(10):951–60. doi: 10.1001/jama.2020.15543

Funding

The study was supported by Shenzhen Science and Technology Plan Project Key Technical Tackling Project (JSGG20200225151806035), Shenzhen Science and Technology Plan General Project (JCYJ20210324131203011).

Conflict of interest

The authors declare that the research was conducted in the absence of any commercial or financial relationships that could be construed as a potential conflict of interest.

Publisher's note

All claims expressed in this article are solely those of the authors and do not necessarily represent those of their affiliated organizations, or those of the publisher, the editors and the reviewers. Any product that may be evaluated in this article, or claim that may be made by its manufacturer, is not guaranteed or endorsed by the publisher.

- Shengyong X, Qiubin Z, Keli L, Yuan Y, Jun X, Yingping T, et al. Consensus of Chinese emergency experts on emergency management of vaccination adverse events(in Chinese). *Chin J Crit Care* (2021) 2(1):93–100. doi: 10.3969/j.issn.1002-1949.2021.02.001
- Wu F, Zhao S, Yu B, Chen YM, Wang W, Song ZG, et al. A new coronavirus associated with human respiratory disease in China. *Nature* (2020) 579(7798):265–9. doi: 10.1038/s41586-020-2008-3
- Rowe M, Melnick J, Gerwien R, Legutki JB, Pfeilsticker J, Tarasow TM, et al. An ImmunoSignature testdistinguishes trypanosoma cruzi, hepatitis b, hepatitis c and West Nile virus seropositivity among asymptomatic blood donors. *PloS Negl Trop Dis* (2017) 11(9):e0005882. doi: 10.1371/journal.pntd.0005882
- Sun P, Ju H, Liu Z, Ning Q, Zhang J, Zhao X, et al. Bioinformatics resources and tools for conformational b-cell epitope prediction. *Comput Math Methods Med* (2013) 2013:943636. doi: 10.1155/2013/943636
- Huang J, Ru B, Dai P. Bioinformatics resources and tools for phage display. *Molecules* (2011) 16(1):694–709. doi: 10.3390/molecules16010694
- Choi YK, Cao Y, Frank M, Woo H, Park SJ, Yeom MS, et al. Structure, dynamics, receptor binding, and antibody binding of the fully glycosylated full-length SARS-CoV-2 spike protein in a viral membrane. *J Chem Theory Comput* (2021) 17(4):2479–87. doi: 10.1021/acs.jctc.0c01144
- Touw WG, Baakman C, Black J, Beek TAH, Krieger E, Joosten RP. Vriend G.A series of PDB-related databanks for everyday needs. *Nucleic Acids Res* (2015) 43(Database issue):D364–8. doi: 10.1093/nar/gku1028
- Kabsch W, Sander C. Dictionary of protein secondary structure: pattern recognition of hydrogen-bonded and geometrical features. *Biopolymers* (1983) 22(12):2577–637. doi: 10.1002/bip.360221211
- Halperin I, Wolfson H, Nussinov R. SiteLight: binding-site prediction using phage display libraries. *Protein Sci* (2003) 12(7):1344–59. doi: 10.1110/ps.0237103
- Ashour HM, Elkhatib WF, Rahman MM, Elshabrawy HA. Insights into the recent 2019 novel coronavirus (SARS-CoV-2) in light of past human coronavirus outbreaks. *Pathogens* (2020) 9(3):186. doi: 10.3390/pathogens9030186
- Luo GG, Gao SJ. Global health concerns stirred by emerging viral infections. *J Med Virol* (2020) 92(4):399–400. doi: 10.1002/jmv.25683

20. Dai L, Gao GF. Viral targets for vaccines against COVID-19. *Nat Rev Immunol* (2021) 21(2):73–82. doi: 10.1038/s41577-020-00480-0
21. Wei J, Stoesser N, Matthews PC, Ayoubkhani D, Studley R, Bell I, et al. COVID-19 infection survey team. Antibody responses to SARS-CoV-2 vaccines in 45,965 adults from the general population of the united kingdom. *Nat Microbiol* (2021) 6(9):1140–9. doi: 10.1038/s41564-021-00947-3
22. Sauré D, O’Ryan M, Torres JP, Zuniga M, Santelices E, Basso LJ. Dynamic IgG seropositivity after rollout of CoronaVac and BNT162b2 COVID-19 vaccines in Chile: a sentinel surveillance study. *Lancet Infect Dis* (2022) 22(1):56–63. doi: 10.1016/S1473-3099(21)00479-5
23. Jiang R, Dou X, Li M, Wang E, Hu J, Xiong D, et al. Dynamic observation of SARS-CoV-2 IgM, IgG, and neutralizing antibodies in the development of population immunity through COVID-19 vaccination. *J Clin Lab Anal* (2022) 36(4):e24325. doi: 10.1002/jcla.24325
24. Arvey A, Rowe M, Legutki JB, An G, Gollapudi A, Lei A, et al. Age-associated changes in the circulating human antibody repertoire are upregulated in autoimmunity. *Immun Ageing*. (2020) 17:28. doi: 10.1186/s12979-020-00193-x
25. Stafford P, Halperin R, Legutki JB, Magee DM, Galgiani J, Johnston SA. Physical characterization of the “immunosignaturing effect”. *Mol Cell Proteomics* (2012) 11(4):M1111.011593. doi: 10.1074/mcp.M111.011593
26. Wang H, Wu X, Zhang X, Hou X, Liang T, Wang D, et al. SARS-CoV-2 proteome microarray for mapping COVID-19 antibody interactions at amino acid resolution. *ACS Cent Sci* (2020) 6(12):2238–49. doi: 10.1021/acscentsci.0c00742
27. Legutki JB, Zhao ZG, Greving M, Woodbury N, Johnston SA, Stafford P. Scalable high-density peptide arrays for comprehensive health monitoring. *Nat Commun* (2014) 5:4785. doi: 10.1038/ncomms5785
28. Legutki JB, Johnston SA. Immun signatures can predict vaccine efficacy. *Proc Natl Acad Sci U S A* (2013) 110(46):18614–9. doi: 10.1073/pnas.1309390110
29. Seyran M, Takayama K, Uversky VN, Lundstrom K, Palù G, Sherchan SP, et al. The structural basis of accelerated host cell entry by SARS-CoV-2. *FEBS J* (2021) 288(17):5010–20. doi: 10.1111/febs.15651
30. Chi X, Yan R, Zhang J, Zhang G, Zhang Y, Hao M, et al. A neutralizing human antibody binds to the n-terminal domain of the spike protein of SARS-CoV-2. *Science* (2020) 369(6504):650–5. doi: 10.1126/science.abc6952
31. Amanat F, Thapa M, Lei T, Ahmed SMS, Adelsberg DC, Carreño JM, et al. SARS-CoV-2 mRNA vaccination induces functionally diverse antibodies to NTD, RBD, and S2. *Cell* (2021) 184(15):3936–3948.e10. doi: 10.1016/j.cell.2021.06.005
32. Planas D, Veyer D, Baidaliuk A, Staropoli I, Guivel-Benhassine F, Rajah MM, et al. Reduced sensitivity of SARS-CoV-2 variant delta to antibody neutralization. *Nature* (2021) 596(7871):276–80. doi: 10.1038/s41586-021-03777-9
33. He X, Hong W, Pan X, Lu G, Wei X. SARS-CoV-2 omicron variant: Characteristics and prevention. *MedComm* (2021) 2(4):838–45. doi: 10.1002/mco2.110
34. Winger A, Caspari T. The spike of concern—the novel variants of SARS-CoV-2. *Viruses* (2021) 13(6):1002. doi: 10.3390/v13061002
35. Hastie KM, Li H, Bedinger D, Schendel SL, Dennison SM, Li K, et al. Defining variant-resistant epitopes targeted by SARS-CoV-2 antibodies: A global consortium study. *Science* (2021) 374(6566):472–8. doi: 10.1126/science.abh2315
36. Ostrov DA. Structural consequences of variation in SARS-CoV-2 B.1.1.7. *J Cell Immunol* (2021) 3(2):103–8. doi: 10.33696/immunology.3.085
37. Ray D, Le L, Andricioaei I. Distant residues modulate conformational opening in SARS-CoV-2 spike protein. *Proc Natl Acad Sci U S A* (2021) 118(43):e2100943118. doi: 10.1073/pnas.2100943118
38. Sabir DK. Analysis of SARS-COV2 spike protein variants among Iraqi isolates. *Gene Rep* (2022) 26:101420. doi: 10.1016/j.genrep.2021.101420
39. Cai Y, Zhang J, Xiao T, Lavine CL, Rawson S, Peng H, et al. Structural basis for enhanced infectivity and immune evasion of SARS-CoV-2 variants. *Science* (2021) 373(6555):642–8. doi: 10.1126/science.abi9745
40. Leung K, Shum MH, Leung GM, Lam TT, Wu JT. Early transmissibility assessment of the N501Y mutant strains of SARS-CoV-2 in the united kingdom, October to November 2020. *Euro Surveill* (2021) 26(1):2002106. doi: 10.2807/1560-7917.ES.2020.26.1.2002106
41. Kazybay B, Ahmad A, Mu C, Mengdesh D, Xie Y. Omicron N501Y mutation among SARS-CoV-2 lineages: Insilico analysis of potent binding to tyrosine kinase and hypothetical repurposed medicine. *Travel Med Infect Dis* (2021) 45:102242. doi: 10.1016/j.tmaid.2021.102242
42. Tian F, Tong B, Sun L, Shi S, Zheng B, Wang Z, et al. N501Y mutation of spike protein in SARS-CoV-2 strengthens its binding to receptor ACE2. *Elife* (2021) 10:e69091. doi: 10.7554/eLife.69091
43. Ibarrondo FJ, Fulcher JA, Goodman-Meza D, Elliott J, Hofmann C, Hausner MA, et al. Rapid decay of anti-SARS-CoV-2 antibodies in persons with mild covid-19. *N Engl J Med* (2020) 383(11):1085–7. doi: 10.1056/NEJMc2025179
44. Cañete PF, Vinuesa CG. COVID-19 makes b cells forget, but T cells remember. *Cell* (2020) 183(1):13–5. doi: 10.1016/j.cell.2020.09.013
45. Kaneko N, Kuo HH, Boucay J, Farmer JR, Allard-Chamard H, Mahajan VS, et al. Loss of bcl-6-Expressing T follicular helper cells and germinal centers in COVID-19. *Cell* (2020) 183(1):143–57. doi: 10.1016/j.cell.2020.08.025
46. Inoue T, Moran I, Shinnakasu R, Phan TG, Kurosaki T. Generation of memory b cells and their reactivation. *Immunol Rev* (2018) 283(1):138–49. doi: 10.1111/imr.12640
47. Ionescu L, Urschel S. Memory b cells and long-lived plasma cells. *Transplantation* (2019) 103(5):890–8. doi: 10.1097/TP.0000000000002594
48. Xia S, Zhang Y, Wang Y, Wang H, Yang Y, Gao GF, et al. Safety and immunogenicity of an inactivated SARS-CoV-2 vaccine, BBIBP-CorV: a randomised, double-blind, placebo-controlled, phase 1/2 trial. *Lancet Infect Dis* (2021) 21(1):39–51. doi: 10.1016/S1473-3099(20)30831-8
49. Peng M, Liu X, Li J, Ren D, Liu Y, Meng X, et al. Successful management of seven cases of critical COVID-19 with early noninvasive-invasive sequential ventilation algorithm and bundle pharmacotherapy. *Front Med* (2020) 14(5):674–80. doi: 10.1007/s11684-020-0796-3
50. Du Y, Lv Y, Zha W, Zhou N, Hong X. Association of body mass index (BMI) with critical COVID-19 and in-hospital mortality: A dose-response meta-analysis. *Metabolism* (2021) 117:154373. doi: 10.1016/j.metabol.2020.154373
51. Soeroto AY, Soetedjo NN, Purwiga A, Santoso P, Kulsum ID, Suryadinata H, et al. Effect of increased BMI and obesity on the outcome of COVID-19 adult patients: A systematic review and meta-analysis. *Diabetes Metab Syndr* (2020) 14(6):1897–904. doi: 10.1016/j.dsx.2020.09.029